NUMERICAL STUDY OF INSTABILITIES IN SEPARATED–REATTACHED FLOWS

Z. YANG
Department of Engineering and Design, University of Sussex, UK.

ABSTRACT

Transition process in separated–reattached flows plays a key role in many practical engineering applications. Hence, accurately predicting transition is crucial since the transition location has a significant impact on the aerodynamic performance and a fundamental understanding of the instability mechanisms involved in transition process is required in order to make significant advances in engineering design and transition control, for example, to delay the turbulent phase where laminar flow characteristics are desirable (low friction drag) or to accelerate it where high mixing of turbulent flow are of interest (in a combustor). The current understanding of instabilities involved in the transition process in separated–reattached flows is far from complete and it is usually very difficult to theoretically and experimentally study the transition process since theoretical studies suffer from the limitation imposed by nonlinearity of the transition process at later stages and experimental studies are limited by temporal and spatial resolution; hence, a thorough description of the transition process is lacking. Nevertheless, significant progress has been made with the simulation tools, such as large eddy simulation (LES), which has shown improved predictive capabilities and can predict transition process accurately. This paper will first briefly present LES formalism followed by its applications to study the transition process in separated–reattached flows, reviewing our current understanding of several important phenomena associated with the transition process and focusing on the instabilities in particular.

Keywords: Instability, large eddy simulation, separated–reattached flows, transition process.

1 INTRODUCTION

Transition from laminar to turbulence in separated–reattached flows occurs very often and plays an important role in many engineering applications from cooling of small electronic devices to airfoil and turbo-machinery design. Laminar boundary layer separation occurs in many engineering problems due to curvature changes or an adverse pressure gradient, such as low Reynolds number flow over aerofoils and turbo-machinery flow. When a laminar boundary layer separates, the free-shear layer formed is inviscidly unstable and has a tendency to undergo transition to turbulence even at relatively low Reynolds numbers. The location where transition starts and the spatial extent within which transition takes place are of crucial interest in engineering design and performance prediction applications.

Laminar-to-turbulence transition has been experimentally and theoretically studied for many decades. A good knowledge with respect to the parameters influencing transition in separated–reattached flows along with indications for related physical mechanisms has been obtained from experimental studies. However, such data can only provide limited temporal and spatial resolution of flow parameters simultaneously, and hence a thorough description of the transition process is lacking. Theoretical studies, on the other hand, suffer from the limitation imposed by nonlinearity of the transition process at later stages. As a result, numerical tools have been applied to study transition. Conventional Reynolds-averaged Navier–Stokes (RANS) approach, based on solving the time- or ensemble-averaged governing equations and hence the effect of all the scales of instantaneous turbulent motion is modelled, is most commonly applied to the solution of engineering turbulent flow problems but is not adequate to predict transition since it only predicts the time- or ensemble-averaged structure and behaviour

of transitional bubbles. Other approaches, such as the semi-empirical e^n method and correlations, are also of limited accuracy and non-universal [1].

One alternative promising approach is large eddy simulation (LES), which was proposed as early as 1963 by Smagorinsky [2]. LES does not adopt the conventional time- or ensemble-averaging RANS approach. In LES, the large-scale motions (large eddies) of turbulent flow are computed directly and only small-scale (sub-grid scale [SGS]) motions are modelled. LES is more accurate than the RANS approach since the larger eddies contain most of the turbulent energy and is responsible for most of the turbulent mixing, and LES directly captures these eddies in full detail, whereas they are modelled in the RANS approach. Furthermore, the small scales tend to be more isotropic and homogeneous than the large ones, and thus modelling the SGS motions should be easier than modelling all scales within a single model as in the RANS approach. However, LES has received increased attention in the engineering community only since 1990s, although it was proposed nearly half a century ago, mainly due to the lack of sufficient computational power since LES requires three-dimensional (3D) time-dependent calculations with small time steps and reasonably fine meshes.

Extensive research has been carried out for attached boundary layer transition and the transition process is generally better understood, which can be divided into the following several stages [3]:

1. Receptivity stage – how the disturbances are projected into growing eigenmodes, or how they enter or otherwise induce disturbances in a boundary layer.
2. Linear growth stage – small disturbances are amplified due to a so-called primary instability of the flow till they reach a size where nonlinear growth starts. This amplification can be in the form of exponential growth of eigenmodes, nonmodal growth of optimal disturbances or nonmodal responses to forcing.
3. Secondary instability – usually once a disturbance reaches a finite amplitude, it often saturates and transforms the flow into a kind of new, possibly steady state. Very rarely the primary instability can lead the flow directly in a turbulent state and the new steady- or quasi-steady flow becomes a base on which secondary instability can occur. This secondary instability can be viewed as a new instability of a more complicated flow.
4. Breakdown stage – nonlinearities and possibly higher instabilities excite an increasing number of scales and frequencies in the flow. This stage is more rapid than both the linear stage and the secondary instability stage.

However, for separated boundary layer flow, the transition process is less understood compared with the attached boundary layer transition. The current paper first briefly presents LES formalism followed by its applications to study unsteady behaviours of transitional separated–reattached flows, focusing on the current understanding of instabilities involved in the transition process.

2 LARGE EDDY SIMULATIONS

2.1 LES governing equations

In LES, only large eddies (large scale motions) are computed directly and hence a low-pass spatial filter (equivalent to a kind of spatial averaging in the form of a convolution with a spatial filter G, separating the flow into grid-resolved scale and SGS) is applied to the

instantaneous conservation equations to formulate the 3D unsteady governing LES equations. The instantaneous velocity can be expressed as:

$$u_i = \overline{u}_i + u'_i \tag{1}$$

where $\overline{u}_i$ is the filtered or resolved scale velocity and u'_i is the SGS velocity and:

$$\overline{u}_i = \int_D u_i G(\xi, \Delta) d^3 \xi \tag{2}$$

where G is a filter function or convolution kernel for which:

$$\int_D G(\xi, \Delta) d^3 \xi = 1 \tag{3}$$

Δ is a characteristic scale of G, referred to as the filter width, and D is the computational domain. Conventionally, it is assumed that the filter width is the same as the cell size. When the finite volume method is employed to numerically solve the LES equations, the equations are integrated over control volumes, equivalent to convolution with a top-hat filter; therefore, there is no need to explicitly apply a filter to the instantaneous equation and in this case it is called *implicit filtering*.

The filtered equation expressing conservation of mass and momentum in a Newtonian incompressible flow can be written in conservative form as:

$$\partial_i \overline{u}_i = 0 \tag{4}$$

$$\rho \partial_t (\overline{u}_i) + \rho \partial_j (\overline{u_i u_j}) = -\partial_i \overline{p} + 2\partial_j (\mu \overline{S}_{ij}) - \partial_j (\tau_{ij}) \tag{5}$$

where the bar over the variables denotes the filtered or resolved scale quantity as introduced before and:

$$\overline{S}_{ij} = \frac{1}{2}(\partial_i \overline{u}_j + \partial_j \overline{u}_i) \tag{6}$$

$$\tau_{ij} = \rho(\overline{u_i u_j} - \overline{u_i}\,\overline{u_j}) \tag{7}$$

$\overline{S}_{ij}$ is the resolved scale strain rate tensor and τ_{ij} is the unknown SGS or residual stress tensor, representing the effects of the SGS motions on the resolved fields of the LES, which must be modelled or approximated using a SGS model.

2.2 SGS modelling

As mentioned above, the SGS stress tensor is unknown and needs to be modelled, which is considered a very important part of LES technique as it can significantly affect the cost and the accuracy of the simulation. The main function of a SGS model is to correctly model the energy transfer between the resolved scale motions and the SGS motions. Many different kinds of SGS models have been developed [4–6] and most of them make an eddy-viscosity assumption (Boussinesq hypothesis) to model the SGS stress tensor as follows:

$$\tau_{ij} = -2\mu_t \overline{S}_{ij} + \frac{1}{3}\delta_{ij}\tau_{ll} \tag{8}$$

μ_t is called SGS eddy viscosity and eqn (5) then becomes:

$$\rho\partial_t(\overline{u_i}) + \rho\partial_j(\overline{u_i u_j}) = -\partial_i\overline{P} + 2\partial_j[(\mu + \mu_t)\overline{S_{ij}}] \tag{9}$$

It should be noted that a modified pressure, $\overline{P} = \overline{p} + 1/3\,\tau_{ll}$, has been introduced and hence when the above equation is solved the pressure obtained is not just the static pressure only. The remaining task now is how to determine the SGS eddy viscosity and the most basic model is the one originally proposed by Smagorinsky [2]:

$$\mu_t = \rho(C_S\overline{\Delta})^2 S \qquad S = (2\overline{S_{ij}\,S_{ij}})^{\frac{1}{2}} \qquad \Delta = (\Delta x\Delta y\Delta z)^{\frac{1}{3}} \tag{10}$$

C_s is the Smagorinsky constant and a typical value of 0.1 is usually used.

Despite increasing interest in developing more advanced SGS models, this very simple model is still very popular because of its robustness, and it is relatively simple to use in simulations and has been used widely and proved surprisingly successful as long as the computational mesh is reasonably fine. However, it has clear shortcomings such as that it is too dissipative (not good for transition simulation) and the Smagorinsky constant needs to be adjusted for different flows. An improvement on this simple SGS model was suggested by Germano *et al*. [7] – a dynamic SGS model, which allows the model constants C_s to be determined locally in space and in time during the simulation. Nevertheless, Reynolds number in representative engineering flows is usually quite high and hence it would be very expensive if a fine mesh is used or when very fine mesh cannot be afforded. Therefore the SGS modelling of small-scale turbulence is of primary importance in LES for industrial flows, especially at high Reynolds numbers and when relatively coarse grids have to be used. Therefore, there is a great need to develop advanced SGS models that are capable of handling practical engineering turbulent flow at high Reynolds numbers since all current available SGS models are not satisfactory when coarse mesh is used in LES.

2.3 Numerical methods

The finite volume approach is very popular in fluid flow simulation and most of LES studies have been carried out using this method. Since many of the numerical issues have been well described, a very brief discussion on spatial and temporal discretization is presented here and the focus will be on one of the most important area in LES: inlet boundary conditions.

2.3.1 Spatial and temporal discretization
One of the most popular spatial discretization scheme used in LES is the second-order central differencing duo to its non-dissipative and conservative properties (not only mass and momentum but also kinetic energy conserving), which are essential for LES. This is the reason why usually first- and second-order upwind schemes or any upwind-biased schemes are not used in LES since they produce too much numerical dissipation. While higher-order numerical schemes, generally speaking, are desirable and can be fairly and easily applied in simple geometries, their use in complex configurations is rather difficult. In addition, it is difficult, at least for incompressible flows, to construct high-order energy conserving schemes. Hence, it is likely that with increasing applications of LES to flows of engineering interest in complex geometries, the second-order central differencing scheme is still going to be wisely used.

As for the temporal discretization (time advancement), implicit schemes allow larger time steps to be used. However, they are more expensive because at each time step nonlinear equations have to be solved. Furthermore, large time steps are unlikely to be used in LES in order to resolve certain time scales for accurate simulations of turbulence. Hence, explicit schemes seem to be more suitable for LES than implicit schemes and most researchers in LES use explicit schemes, such as the second-order Adams–Bashforth scheme. Since the time steps are usually small in LES, it is not essential to use higher-order schemes either.

2.3.2 Inflow boundary conditions

Accurately specifying inlet conditions for LES is of extreme importance since, in many cases, the downstream flow development within the domain is largely determined by the inlet behaviour. However, it is a very difficult task to accurately generate inlet boundary conditions in LES. This is because in LES at inflow boundary, unlike the RANS computations where only time-averaged information is required that can be usually specified according to experimental data, three components of instantaneous velocity need to be specified at each time step, which should posses characteristics, such as stochastically varying, with scales down to the filter scale (spatially and temporally), compatible with the Navier–Stokes equations and turbulent structures (turbulence intensities, length scales, spectrum etc.). Hence, it is extremely hard to generate inlet boundary conditions in LES which have all the characteristics listed above, especially with turbulent structures since it is possible to generate a wide range of flow fluctuations around the mean which may have specified spectral properties, such as intensity and length scales, and even compatible with the Navier–Stokes equations. However, those generated flow fluctuations may not have the structure of turbulence, of coherent eddies across a range of spatial scales down to the Kolmogorov scale which interact with each other. It is also worth pointing out that turbulent structures are different between free stream turbulence (FST) and wall-bounded turbulence, when generating inflow boundary conditions in LES.

Existing methods for inflow boundary conditions in LES can be classified into two basic categories: the so-called precursor simulation technique which is to basically perform another simulation and store the data as the input for the required simulation, and synthesis methods in which some form of random fluctuation is generated and combined with the mean flow at the inlet. Precursor method can generate the most realistic turbulence information at inflow boundary but the disadvantage is the necessity to set up and run a separate calculation, leading to usually very high computational cost. In order to save computational cost there is actually no reason why the precursor calculation cannot be integrated into the main domain, with sampling downstream of the inlet being mapped back into the inlet. It is, of course, necessary to provide some mechanism for driving the flow towards a pre-specified target, such as mean velocity profiles and turbulent stresses, etc., by recycling and rescaling. This method, which was first developed for flat-plate boundary layers, consists of taking a plane of data from a location several boundary-layer thicknesses downstream of the inflow, and separately rescaling the inner and outer layers of velocity profiles, to account for the different similarity laws that are observed in these two regions. The rescaled velocity profiles are then reintroduced at the inlet. The main shortcoming is that the inlet must be placed in a region in which the flow is in an equilibrium or very slowly developing, well-known condition (mean velocity and turbulent quantities) and a fairly long domain must be used for the region of interest for the recycling.

There are many synthesis generation methods developed and the most basic way is to specify the mean flow velocity profile (usually obtained experimentally) plus some random perturbations, for example, adding a white-noise random component to the mean velocity at inlet, with an amplitude determined by the turbulent intensity level. This simplest method is not a good one at all since the white noise component has hardly any of the required characteristics of turbulent flow – in particular it possesses no spatial or temporal correlations at all. Therefore, they rapidly decay and it usually takes a long distance downstream from the inflow boundary for a desired realistic turbulence to develop, and in some cases the use of random noise at the inlet does not develop turbulence at all. Significant efforts have been made to develop more advanced synthesis techniques generating fluctuations which are more realistic and must involve introducing spatial and/or temporal correlation. So far many advanced synthesis generation methods have been developed and can be broadly classified into four categories: Fourier techniques [8] and related approaches; principal orthogonal decomposition methods [9]; digital filter generation methods [10] and finally vortex method [11] or synthetic eddy method. Details on inlet boundary condition generation methods can be found in a review article [12]. However, so far all those developed methods mentioned above can only generate inflow turbulence with certain properties but no methods are available yet to generate inflow turbulence with all the desired characteristics, such as intensity, shear stresses, length scales and power spectrum.

3 APPLICATIONS OF LES TO STUDY TRANSITION PROCESS

This section presents a brief overview of LES studies of transition process in separated–reattached flows and tries to summarize the current understanding of the transition process, focusing mainly on flow instability (primary and secondary instabilities) and several important flow phenomena associated with the transition process.

3.1 Primary instability

Many previous studies have stated that in the absence of any finite magnitude environmental disturbances, transition in the separated shear layer of a separation bubble is normally initiated through the inviscid Kelvin–Helmholtz (KH) instability mechanism. This mode of instability closely resembles that of the planar free-shear layer in mixing layers and jets [13]. However, there had been no vigorous proof that the primary instability in the transition process of separated–reattached flows was indeed the KH instability till the LES study of Yang and Voke [14] which gave vigorous evidence that a primary 2D instability of a separated shear layer (induced by a smooth leading edge) was via the KH mechanism. To clearly illustrate this point, it is useful to briefly review what the KH instability is and how Yang and Voke's study revealed that it was the KH instability in the separated boundary layer transition on a flat plate with a semi-circular leading edge.

The KH instability was originally derived from two parallel stream of fluids with different velocities (U_1 and U_2) and densities mixing at certain point. A free-shear layer is formed with discontinuities in density and velocity at the interface. If the density of the upper stream is less than the density of the lower stream, the arrangement is a stable one when the velocity difference between the upper stream and the lower stream is zero ($U_2 - U_1 = 0$). However, for a given difference in velocity ($U_2 - U_1 > 0$, or $U_2 - U_1 < 0$), no matter how small this difference is, instability occurs for disturbances with all wave numbers larger than a critical value (for disturbances of sufficiently small wavelengths). It can also be stated that for a

given waver number, instability would occur if the velocity difference, $U_2 - U_1$, is larger than a threshold. This instability is called the KH instability. Chandrasekhar [15] considered the case of continuous variation of velocity and certain distribution of ρ (characterized by the Richardson number) and concluded from the inviscid linear stability analysis that, for any values of the Richardson number, there are always bands of wavelengths for which the KH instability occurs. In particular, when the Richardson number is zero, that is, for constant density, the condition for the KH instability to occur is $0 < Kh < 1.2785$, where K is the wave number and h is the shear layer thickness.

Yang and Voke [14] extracted both K and h from the LES data in a separated boundary layer transition study on a flat plate with a semi-circular leading edge and worked out a value $Kh = 0.984$ (h is the shear layer thickness where the unsteadiness first becomes apparent and the wave number is worked out using $K = 2\pi f/c$, f is the characteristic frequency which is obtained from the spectra analysis and c is the wave speed equal to the velocity at the critical layer, that is, the streamwise velocity at the inflection point). This value (0.984) satisfies the above KH instability criterion. Abdalla and Yang [16] in their LES studies of a transitional separation bubble over a flat plate with a blunt leading edge obtained $Kh = 1.1245$, which again satisfies the above KH instability criterion, hence they concluded that the free-shear layer in separated boundary layer transition over a flat plate with two different leading edges becomes unstable via the same instability, KH instability.

Many other studies have also shown that the KH instability plays a dominant role in the transition process of separation bubbles and it is generally now believed that the primary instability in the free-shear layer of a separation bubble is the KH instability. However, the LES study by Roberts and Yaras [17] demonstrated that transition in a separation bubble through the KH instability does not eliminate the existence of the Tollmien–Schlichting (TS) instability (a viscous instability typically associated with attached flow boundary layer transition) in the inner part of the flow where the roll up of shear layer into vortical structures occurred at the dominant TS frequency. They emphasized the possibility of an interaction between the TS and the KH instability modes. This was also observed from the coarse direct numerical simulation study by McAuliffe and Yaras [18] on transition of a bubble formed due to adverse pressure gradient that the transition process in the separation bubbles shared features from both attached boundary layer (the TS instability) and free-shear layer (the KH instability). A few experimental studies have also suggested that the TS instability mechanism may play a significant role in the breakdown to turbulence in a separation bubble [19–21].

3.2 Secondary instability

In attached boundary layer transition, it is well known that after the primary instability stage the initial small disturbances grow to finite amplitudes, which may saturate to a steady state (or quasi-steady state) and establish a new, usually more complicated, mean flow. This mean flow in turn may become unstable to infinitesimal disturbances due to a so-called secondary instability. The secondary instability mechanisms are reasonably well understood for attached boundary layer transition, such as K-type secondary instability, H-type secondary instability or O-type secondary instability [3], but for the transition process in a separation bubble after the primary KH instability stage, the secondary instability mechanisms are much less understood. In a temporally growing mixing layer Metcalfe *et al.* [22] carried out detail numerical studies on secondary instability and clearly demonstrated that there were two secondary
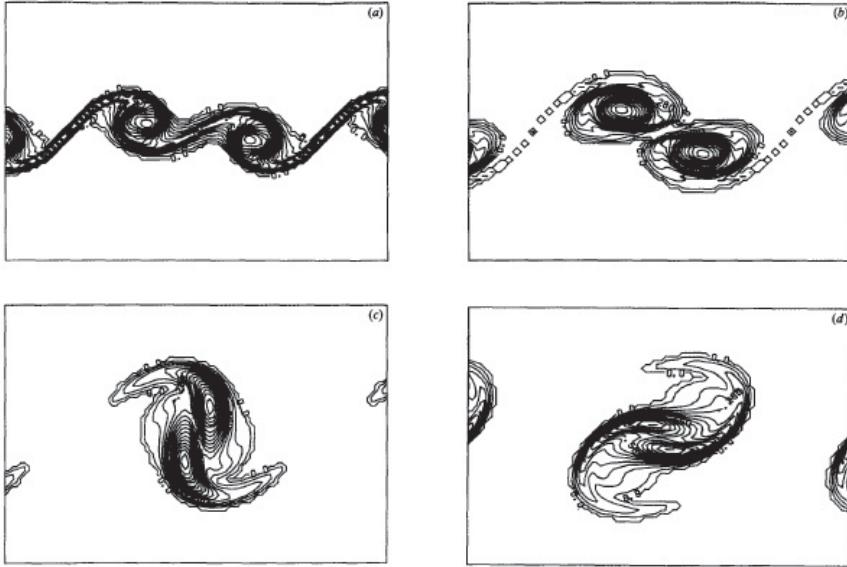
Figure 1: Instantaneous spanwise vorticity contours showing a vortex pairing process in a mixing layer: (a) $t = 8$, (b) $t = 16$, (c) $t = 24$, (d) $t = 32$ (courtesy of Metcalfe *et al.*).

instabilities involved: a 2D sub-harmonic secondary instability, also called a 2D sub-harmonic pairing mode (pairing instability) as this involves roll-up and pairing of spanwise vortices; a 3D secondary instability (3D mode) and once the 3D disturbance reaches a finite amplitude, it produces bending of the core of the spanwise rollers, leading to the so called rib vortices extending in the streamwise direction. Figure 1 shows a vortex paring process in the mixing layer study by Metcalfe *et al.* [22]. Several other studies also indicated that the flow after the KH instability does undergo a secondary instability leading to the vortex pairing phenomenon in planar free-shear layers [13,23,24]. Those two secondary instabilities may coexist and compete, and which secondary instability is at work or more dominant significantly depends on flow history such as the initial disturbances, the relative amplitudes of each mode and the external environment in which the flow embedded etc. It was shown [22] that the roll-up and pairing of the 2D modes has a stabilizing effect on the higher wavenumber spanwise modes and on the overall 3D growth rate when the amplitude of the 3D modes is small, while the absence of pairing (saturation) can enhance the 3D growth rate.

A similar vortex pairing phenomenon has been reported in a study on transition in a separation bubble [25]. McAuliffe and Yaras [26] carried out a thorough experimental study on the nature of transition in a separation bubble and manipulations of the resultant breakdown to turbulence through passive means of control. The vortex pairing phenomenon initiated by a sub-harmonic instability as mentioned before was clearly observed in their particle image velocimetry measurements as shown in Fig. 2 through a series of *x–y* plots of normalized spanwise vorticity. At $t^* = 0$, a large vortex resulting from roll-up of the separated shear layer appears, followed later on by a second upstream vortex, identified by a region of concentrated negative vorticity, entering the field of view at $t^* = 0.0544$, and the sub-harmonic instability causes it to shift towards the higher-velocity side of the shear layer. As this upstream vortex travels downstream at a higher speed and catches up to the first vortex
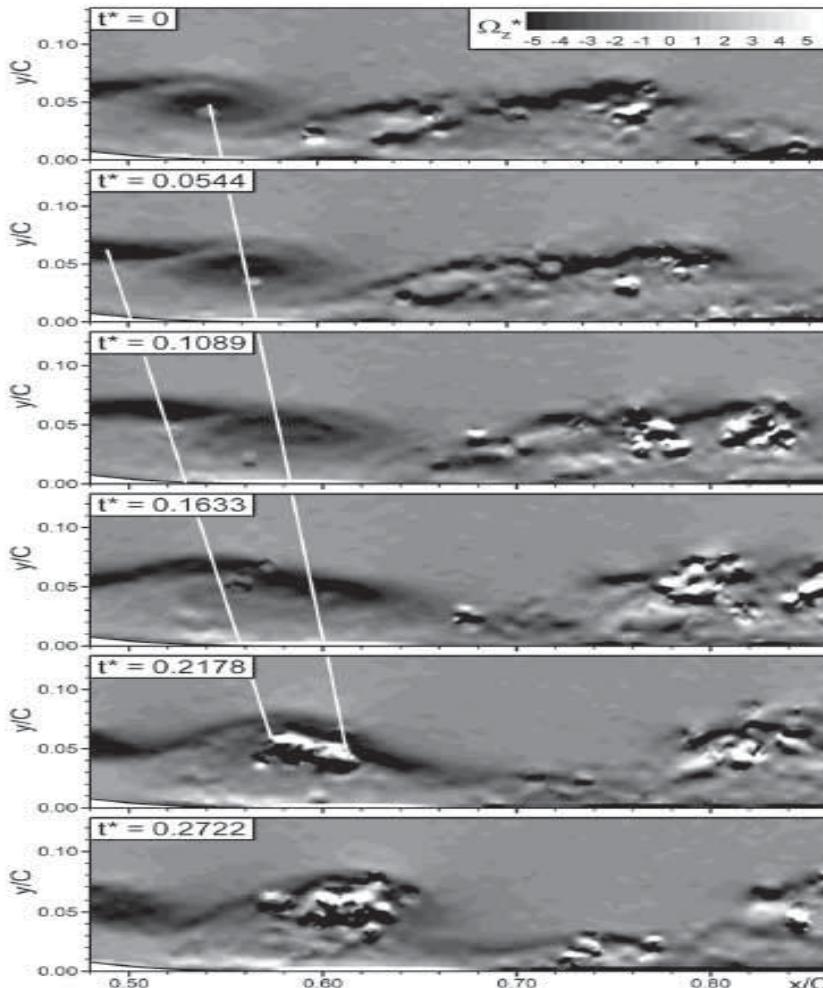
Figure 2: Instantaneous spanwise vorticity showing the vortex pairing phenomenon in a transitional separation bubble (courtesy of McAuliffe and Yaras).

downstream, the two vortices become stretched and elongated as they rotate about each other due to mutual induction of their vorticity fields and subsequently merge into a single vortex structure. The trajectories of the two vortex cores are clearly observed in the figure, showing the difference in convection rates of the two vortices due to the sub-harmonic instability. When the vortices merge, the production of smaller-scale turbulence is observed near the core of the new vortex, indicated by the stronger vorticity fluctuations, and at $t^* = 0.2722$ the new vortex is dominated by small-scale fluctuations. During the vortex pairing process, the resultant stronger new vorticies have approximately double the spacing of the primary vortices – hence the identification of this process as a sub-harmonic of the primary instability. Abdalla and Yang [16] carried out an LES study of the primary and secondary instabilities of a separated boundary layer transition on a flat plate with a blunt leading edge, demonstrating that a similar sub-harmonic secondary instability was present as a vortex pairing process was observed. Figure 3 shows large-scale flow structures present in the
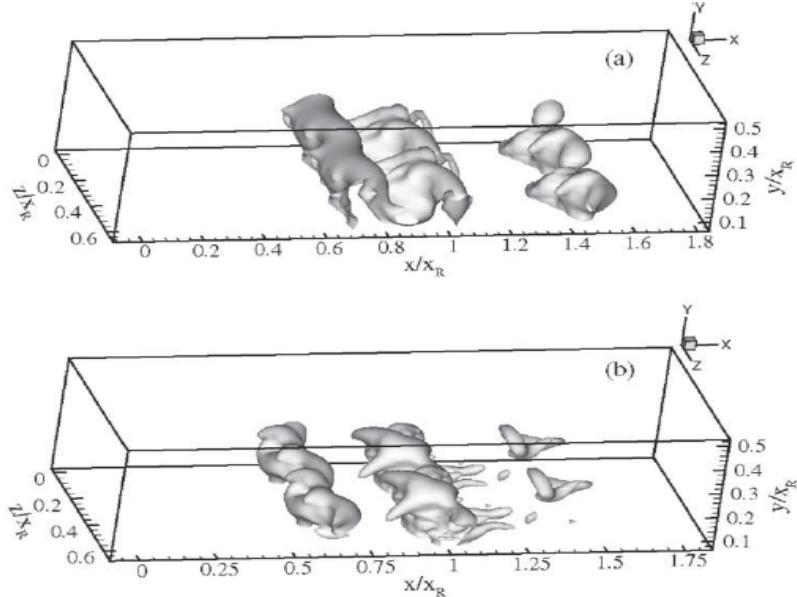
Figure 3: Instantaneous low-pressure isosurfaces showing the vortex pairing phenomenon in a transitional separation bubble.

separated boundary layer transition [16] and it can be seen from Fig. 3a that two spanwise vortices are about to merge at a normalized $t = 322.3$. Figure 3b shows that at $t = 390.2$, the structures most likely consist of two spanwise vortices as a result of the pairing process.

However, this pairing process has been only captured very rarely among the extensive data analysed by Abdalla and Yang [16], indicating that although the sub-harmonic secondary instability is present, it may not be the dominant one and a 3D secondary instability, as mentioned above, could be present too and compete against the pairing instability. Figure 4 confirms that a 3D secondary instability is, indeed, present as the characteristic features of the 3D secondary instability, the so-called rib vortices extending in the streamwise direction can be clearly seen in Fig. 4a and b. Nevertheless, it is very difficult to pinpoint which secondary instability is more dominant. It is worth pointing out that the discussion so far is related to transition under low FST, and when the FST increases above certain level, the transition process could be different, which will not be covered in the present paper and will be only very briefly discussed in the following paragraph.

In summary, our current understanding of the transition process in separated–reattached flows is:

1. a primary 2D instability (mostly KH instability),
2. followed by secondary instability (a sub-harmonic pairing stability and/or a 3D instability), and
3. a breakdown stage where fully turbulent flow emerges.

Another key parameter affecting the transition process of a transitional separation bubble and its following reattachment is FST. Experimental studies have demonstrated that FST increases
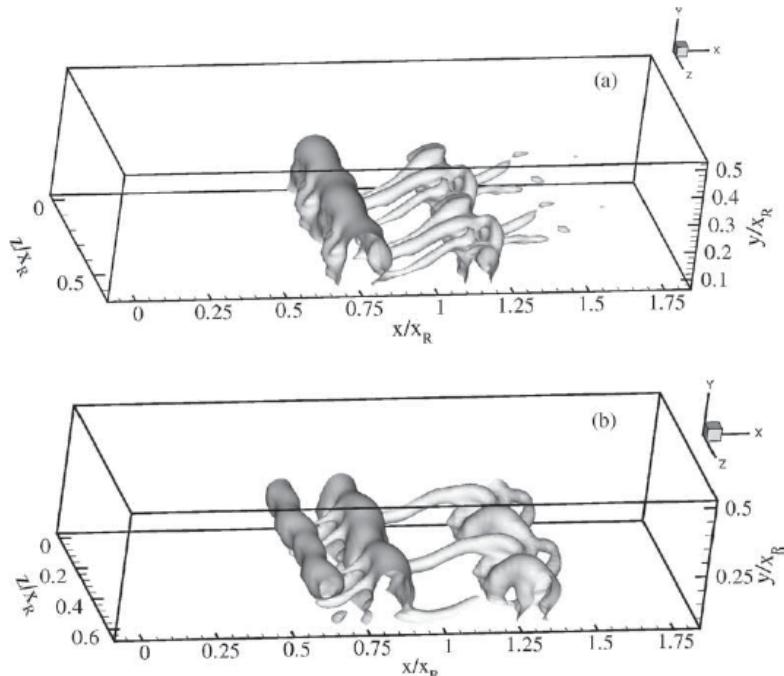
Figure 4: Instantaneous low-pressure isosurfaces showing the so-called rib vortices in a transitional separation bubble.

the shear-layer entrainment rates, decreases the mean reattachment length and results in an earlier transition to turbulence. Yang and Abdalla [27,28] performed LES studies of separated boundary layer transition under 2% FST. They reported a 14% reduction of the mean bubble length and an earlier breakdown of the free-shear layer compared with the zero FST case. At 2% FST, 2D KH rolls were not as apparent as in the case with zero FST, but still coherent 2D structures (spanwise vortices) in the early part of the bubble were observable. The 3D lambda-shaped vortices could hardly be identified and streamwise structures were enlarged in the spanwise direction and shortened in the streamwise direction compared with the zero FST case. The vortex pairing process and the so-called rib vortices shown in Figs 3 and 4 could be hardly seen in the presence of 2% FST, indicating that secondary instability could be quite different or maybe even bypassed although the primary instability of the free-shear layer was still the same as in the zero FST case (KH instability mechanism). Further increase in FST could change the whole transition process.

3.3 Shedding phenomenon

A very important feature associated with separated–reattached flows is vortex shedding from the free-shear layer of a separation bubble at different frequencies. In a steady laminar separation bubble, one can define a fixed reattachment point or line where the skin friction is zero. However, this is not the case in transitional and turbulent separation bubbles as the instantaneous flow field is highly unsteady around the 'mean' reattachment point and the notion of a reattachment 'point' or 'line' is misleading as it continuously varies with time. It
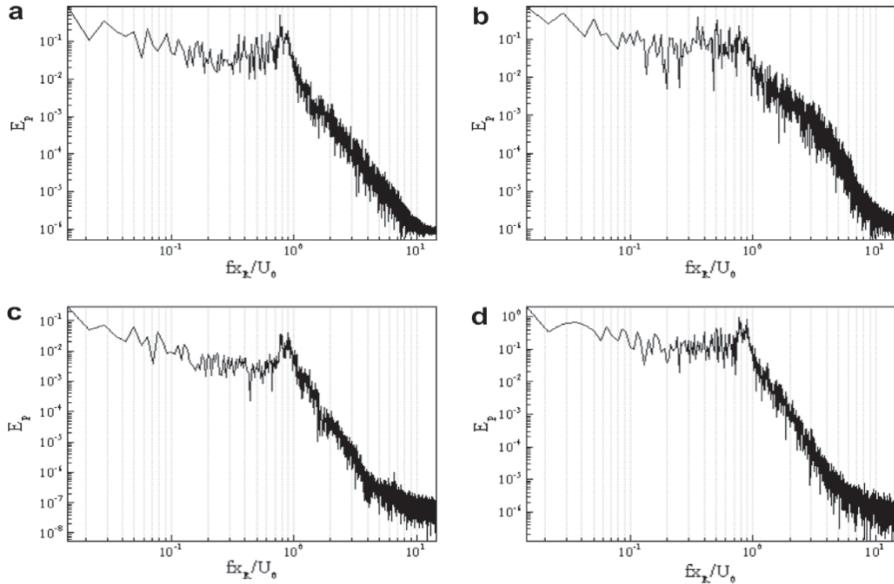
Figure 5: Pressure spectra showing the peak frequency band at $x/x_R = 0.75$ and four vertical locations: $y/x_R = 0.01$(a), $y/x_R = 0.05$(b), $y/x_R = 0.13$(c), $y/x_R = 0.2$(d).

is quite normal that several small bubbles or vortices are formed and then shed afterwards, leading to a vortex shedding phenomenon. Figure 5 shows pressure spectra at several different locations in a separated boundary layer transition on a flat plate with a blunt leading edge [28] and a peak frequency band at about 0.8–0.9 U_0/x_R is clearly observable (U_0 is the free stream velocity and x_R is the mean bubble length). This peak frequency band was also observed in several experimental studies of separated–reattached flow over a plate with a sharp leading edge at high Reynolds number [29–31]. This peak frequency band was stated to be the characteristic frequency of the large vortices shedding from the free-shear layer of the bubble. Furthermore, a low frequency peak (0.12 U_0/x_R) was also reported in those experimental studies near the separation line. This low frequency peak was not clearly understood and was suggested as related to the large-scale shrinkage and enlargement of the bubble. A low frequency peak (0.125–0.2 U_0/x_R) was also observed in the LES study by Yang and Voke [14] on a flat plate with a smooth leading edge and they suggested that this was associated with large shrinkage of the bubble caused by a big vortex shedding at a lower frequency. However, this low frequency peak was not observed in separated boundary layer transition studies on a flat plate with a blunt leading edge at very low FST [32]. Yang and Abdalla [28] studied the same problem with 2% FST and reported a peak frequency band at about 0.8–0.9 U_0/x_R, in close agreement with the characteristic frequencies already measured in previous studies, but again no low frequency peak was observed and further study is needed to clarify this point.

3.4 Coherent structures

Large-scale structures (large-scale organized motions), usually called coherent structures (CS), have been revealed in many experimental studies to dominate the entrainment and
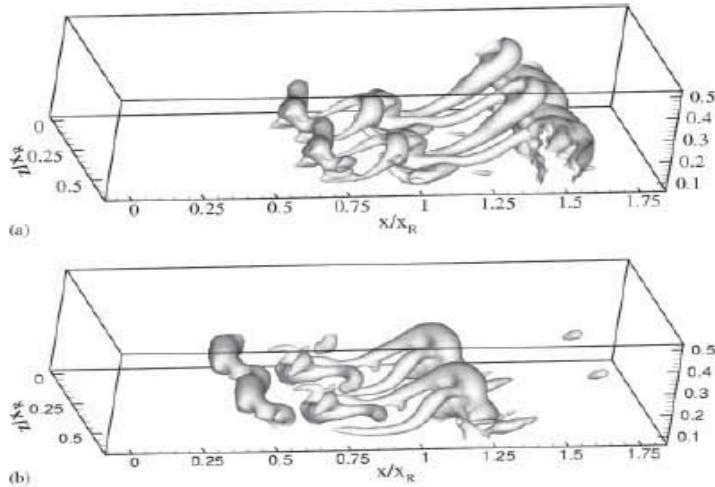
Figure 6: Instantaneous low-pressure isosurfaces showing the evolution of 2D spanwise (KH) rolls into 3D lambda-shaped vortices.

mixing phenomena in free shear flows [33]. It is important to understand the physics of CS so that a better insight into turbulence phenomena can be obtained (such as entrainment and mixing, heat and mass transfer, drag and aerodynamic noise generation, etc.). However, despite considerable usage in the literature it seems that an approved definition for CS does not yet exist. Cantwell [34] describes CS as spatially coherent and temporally evolving vortical structures. *KH rolls*, *Streaks*, *Hairpin vortices (also called Lambda-shaped vortices)* and *ribs* are some of the common large-scale flow structures which are referred to as CS in the literature. Streaky structures are characterized with narrow regions of low velocity fluid stretched in the streamwise direction [35,36]. Streamwise vortices are vortical structures which are predominantly oriented in the streamwise direction, although they may be bent and make an angle with the streamwise direction. Spanwise vortices are referred to as those primarily oriented in the spanwise direction, such as KH rolls. Hairpin vortices (lambda-shaped vortices) are those with two legs of quasi-streamwise vortex pairs with opposite signs and a tip of spanwise vorticity.

CS usually depends on flow geometry, flow condition and location with respect to solid surfaces. Large-scale spanwise vortices in plane mixing layers, lambda-shaped vortices and low-speed streaks in transitional and turbulent boundary layers and counter-rotating vortices in wakes are the dominant structures controlling the flow dynamics. Vortical structures in separated shear layers grow, merge and periodically shed from the reattachment region. KH rolls and lambda-shaped vortices have been observed in separated layer transition as shown in Fig. 6 displaying the evolution of KH rolls into lambda-shaped vortices in a separated boundary layer transition [27], and the transition process is better understood by studying the evolution of KH rolls into lambda-shaped vortices [14,16,37,38]. It is believed that reorientation of vorticity in the streamwise direction is a key mechanism for the reattachment process as it provides enhanced momentum exchange in the wall-normal direction. Abdalla *et al.* [38], in a LES study of transitional separated–reattached flow over a surface-mounted obstacle and a forward-facing step, demonstrated that the CS, such as the lambda-shaped and

rib-like vortices, which are often associated with a flat plate boundary layer and also found in the separated–reattached flow, are not common in the separated–reattached flow over obstacles and forward-facing steps.

4 CONCLUSIONS

A brief LES formalism has been presented and its applications to study transition process in separated–reattached flows, focusing on the current understanding of physics of the transition process, in particular on the primary and secondary instabilities, have been reviewed. Several important issues associated with LES, such as SGS modelling and numerical methods, have been briefly discussed. One of the most important and yet very difficult problem associated with LES is the specification of realistic inflow boundary conditions with proper turbulence characteristics, such as spectrum, length scales etc.; hence, the current status of generation methods for the inflow boundary conditions has been thoroughly reviewed in the present paper.

Significant progress has been made towards a better understanding of the transition process in separated–reattached flows and it is well understood that the free-shear layer formed in the separation bubble becomes initially inviscidly unstable via the KH instability mechanism (primary instability). However, it is not entirely clear about a further instability mechanism (secondary instability) on how these initial 2D instability waves grow downstream and develop into 3D motions and eventually break down to fully turbulent flow. There are evidences suggesting that the transformation of 2D KH rolls into 3D vortical structures may be due to two different secondary instabilities: a kind of 2D sub-harmonic Eckhaus-type secondary instability and a 3D elliptic-type secondary instability. One of those secondary instabilities may be the dominant one in some cases and maybe both of them are equally important in other cases and further studies are needed to clarify this.

Other factors which can influence the transition process in a separated boundary layer, such as FST (both intensity level and length scales), have not been discussed in the present paper and is currently under investigation by the author. The final breakdown stage to turbulence is far from fully understood and further research in this area is much needed.

ACKNOWLEDGEMENT

REFERENCES

[1] Langtry, R.B. & Menter, F.R., Transition modelling for general CFD applications in aeronautics. *AIAA 2005-522*, Reno, Nevada, 2005.

[2] Smagorinsky, J., General circulation experiments with the primitive equations: I – the basic experiment. *Monthly Weather Review*, **91**, pp. 99–164, 1963. doi: http://dx.doi.org/10.1175/1520-0493(1963)091<0099:GCEWTP>2.3.CO;2

[3] Schmid, P.J. & Henningson, D.S., *Stability and Transition in Shear Flows*, Springer: New York, 2001. doi: http://dx.doi.org/10.1007/978-1-4613-0185-1

[4] Lesieur, M. & Metais, O., New trends in large eddy simulations of turbulence. *Annual Review of Fluid Mechanics*, **28**, pp. 45–82, 1996. doi: http://dx.doi.org/10.1146/annurev.fl.28.010196.000401

[5] Sagaut, P., *Large Eddy Simulation for Incompressible Flows: An Introduction*, 2nd edn, Springer: Berlin, 2003.

[6] Kajishima, T. & Nomachi, T., One-equation sub-grid scale model using dynamic procedure for the energy production. *Transaction of ASME*, **73**, pp. 368–373, 2006.

[7] Germano, P., Piomelli, U., Moin, P. & Cabot, W.H., A dynamic sub-grid scale eddy viscosity model. *Physics of Fluids*, **3(7)**, pp. 1760–1765, 1991. doi: http://dx.doi.org/10.1063/1.857955

[8] Lee, S., Lele, S. & Moin, P., Simulation of spatially evolving turbulence and the applicability of Taylor's hypothesis in compressible flow. *Physics of Fluids A*, **4**, pp. 1521–1530, 1992. doi: http://dx.doi.org/10.1063/1.858425

[9] Druault, P., Lardeau, S., Bonnet, J.-P., Coiffet, F., Deville, J., Lamballais, E., et al. Generation of three-dimensional turbulent inlet conditions for large-eddy simulation. *AIAA Journal*, **42(3)**, pp. 447–456, 2004. doi: http://dx.doi.org/10.2514/1.3946

[10] Veloudis, I., Yang, Z., McGuirk, J.J., Page, G.J. & Spencer, A., Novel implementation and assessment of a digital filter based approach for the generation of large-eddy simulation inlet conditions. *Journal of Flow, Turbulence and Combustion*, **79**, pp. 1–24, 2007. doi: http://dx.doi.org/10.1007/s10494-006-9058-y

[11] Benhamadouche, S., Jarrin, N., Addad, Y. & Laurence, D., Synthetic turbulent inflow conditions based on a vortex method for large eddy simulation. *Progress in Computational Fluid Dynamics*, **6(1–3)**, pp. 50–57, 2006. doi: http://dx.doi.org/10.1504/PCFD.2006.009482

[12] Tabor, G.R. & Baba-Ahmadi, M.H., Inlet conditions for large eddy simulation: a review. *Computers & Fluids*, **39**, pp. 553–567, 2010. doi: http://dx.doi.org/10.1016/j.compfluid.2009.10.007

[13] Ho, C.M. & Huerre, P., Perturbed free shear layers. *Annual Review of Fluid Mechanics*, **16**, pp. 365–424, 1984. doi: http://dx.doi.org/10.1146/annurev.fl.16.010184.002053

[14] Yang, Z. & Voke, P.R., Large-eddy simulation of boundary layer separation and transition at a change of surface curvature. *Journal of Fluid Mechanics*, **439**, pp. 305–333, 2001. doi: http://dx.doi.org/10.1017/S0022112001004633

[15] Chandrasekhar, S., *Hydrodynamic and Hydromagnetic Stability*, Clarendon Press: Oxford, 1961.

[16] Abdalla, I.E. & Yang, Z., Numerical study of the instability mechanism in transitional separating-reattaching flow. *International Journal of Heat and Fluid Flow*, **25**, pp. 593–605, 2004. doi: http://dx.doi.org/10.1016/j.ijheatfluidflow.2004.01.004

[17] Roberts, S.K. & Yaras, M.I., Large-eddy simulation of transition in a separation bubble. *ASME Journal of Fluids Engineering*, **128**, pp. 232–238, 2006. doi: http://dx.doi.org/10.1115/1.2170123

[18] McAuliffe, B.R. & Yaras, M.I., Numerical study of instability mechanisms leading to transition in separation bubbles. *ASME Journal of Turbomachinery*, **130**, pp. 1–8, 2008. doi: http://dx.doi.org/10.1115/1.2750680

[19] Lang, M., Rist, U. & Wagner, S., Investigations on controlled transition development in a laminar separation bubble by means of LDA and PIV. *Experiments in Fluids*, **36**, pp. 43–52, 2004. doi: http://dx.doi.org/10.1007/s00348-003-0625-x

[20] Roberts, S.K. & Yaras, M.I., Effects of periodic unsteadiness, free-stream turbulence and flow Reynolds number on separation-bubble transition. *ASME-GT2003-38626*, 2003.

[21] Volino, R.J. & Bohl, D.G., Separated flow transition mechanism and prediction with high and low free stream turbulence under low pressure turbine conditions. *ASME-GT2004-53360*, 2004.

[22] Metcalfe, R.W., Orszag, S.A., Brachet, M.E. & Riley, J.J., Secondary instability of a temporally growing mixing layer. *Journal of Fluid Mechanics*, **184**, pp. 207–243, 1987. doi: http://dx.doi.org/10.1017/S0022112087002866

[23] Huang, L.S. & Ho, C.M., Small-scale transition in a plane mixing layer. *Journal of Fluid Mechanics*, **210**, pp. 475–500, 1990. doi: http://dx.doi.org/10.1017/S0022112090001379

[24] Winant, C.D. & Browand, F.K., Vortex pairing: the mechanism of turbulent mixing-layer growth at moderate Reynolds number. *Journal of Fluid Mechanics*, **63**, pp. 237–255, 1974. doi: http://dx.doi.org/10.1017/S0022112074001121

[25] Malkiel, E. & Mayle, R.E., Transition in a separation bubble. *ASME Journal of Turbomachinery*, **118**, pp. 752–759, 1996. doi: http://dx.doi.org/10.1115/1.2840931

[26] McAuliffe, B.R. & Yaras, M.I., Passive manipulation of separation-bubble transition using surface modifications. *ASME Journal of Fluids Engineering*, **131**, pp. 021201: 1–16, 2009.

[27] Yang, Z. & Abdalla, I.E., Effects of free-stream turbulence on large-scale coherent structures of separated boundary layer transition. *International Journal for Numerical Methods in Fluids*, **49**, pp. 331–348, 2005. doi: http://dx.doi.org/10.1002/fld.1014

[28] Yang, Z & Abdalla, I.E., Effects of free-stream turbulence on a transitional separated-reattached flow over a flat plate with a sharp leading edge. *International Journal of Heat and Fluid Flow*, **30**, pp. 1026–1035, 2009. doi: http://dx.doi.org/10.1016/j.ijheatfluidflow.2009.04.010

[29] Kiya, M. & Sasaki, K., Structure of a turbulent separation bubble. *Journal of Fluid Mechanics*, **137**, pp. 83–113, 1983. doi: http://dx.doi.org/10.1017/S002211208300230X

[30] Cherry, N.J., Hillier, R. & Latour, M.E.M.P., Unsteady measurements in a separating and reattaching flow. *Journal of Fluid Mechanics*, **144**, pp. 13–46, 1984. doi: http://dx.doi.org/10.1017/S00221120840014X

[31] Kiya, M. & Sasaki, K., Structure of large-scale vortices and unsteady reverse flow in the reattaching zone of a turbulent separation bubble. *Journal of Fluid Mechanics*, **154**, pp. 463–491, 1985. doi: http://dx.doi.org/10.1017/S0022112085001628

[32] Abdalla, I.E. & Yang, Z., Numerical study of a separated-reattached flow on a blunt plate. *AIAA Journal*, **43**, pp. 2465–2474, 2005. doi: http://dx.doi.org/10.2514/1.1317

[33] Hussain, A.K.M.F., Coherent structures and turbulence. *Journal of Fluid Mechanics*, **173**, pp. 303–356, 1986. doi: http://dx.doi.org/10.1017/S0022112086001192

[34] Cantwell, B.J., Organised motion in turbulent flow. *Annual Review of Fluid Mech*anics, **13**, pp. 457–515, 1981. doi: http://dx.doi.org/10.1146/annurev.fl.13.010181.002325

[35] Kim, H.T., Kline, S.J. & Reynolds, W.C., The production of turbulence near a smooth wall in a turbulent boundary layer. *Journal of Fluid Mechanics*, **50**, pp. 133–160, 1971. doi: http://dx.doi.org/10.1017/S0022112071002490

[36] Smith, C.R. & Metzler, S.P., The characteristics of low-speed streaks in the near-wall region of a turbulent boundary layer. *Journal of Fluid Mechanics*, **129**, pp. 27–54, 1983. doi: http://dx.doi.org/10.1017/S0022112083000634

[37] Yang, Z., Large-scale structures at various stages of separated boundary layer transition. *International Journal of Numerical Methods in Fluids*, **40**, pp. 723–733, 2002. doi: http://dx.doi.org/10.1002/fld.373

[38] Abdalla, I.E., Yang, Z. & Cook, M., Computational analysis and flow structure of a transitional separated-reattached flow over a surface mounted obstacle and a forward-facing step. *International Journal of Computational Fluid Dynamics*, **23**, pp. 25–57, 2009. doi: http://dx.doi.org/10.1080/10618560802566246